Original Article

ENERGY EXPLORATION & EXPLOITATION

Energy Exploration & Exploitation
0(0) 1–23

DOI: 10.1177/0144598717742969
journals.sagepub.com/home/eea

SAGE

The geochemical characteristics of Tazhong crude oils from the Tarim Basin, northwestern China

Yungan Liang,[1,2] Jianbing Xu,[1,2] Wenwen Li,[3] Bin Cheng,[1] Qian Deng,[1,2] Haizu Zhang[4] and Zewen Liao[1]

Abstract

Recent exploration work in the Tazhong district has gradually transferred to the exploitation of high and over mature oils in deep and ultra-deep layers. This has proved problematic, however, as the distribution of crude oils in the Tazhong is complex. This means that the geochemical characterization of high and over mature oils, especially for light crude oils, have become increasingly important. The stability of concerted ring structure of aromatics makes them having stronger thermal stability and resistance to biodegradation. This means that there are abundant aromatic compounds in high and over mature oils. This study presents a series of geochemical analyses of the maturity parameters of 89 crude oils from the Tazhong area, including stable carbon and hydrogen isotope analyses of compounds from 43 light crude oils. These analyses are then compared with other data from the Tazhong Number I fault zone, as well as the Tazhong Number 10 and Tazhong Uplift structural zones. Results show that the geochemical parameters of oils from Tazhong Number I fault zone generally encompass a wider range than those from the Tazhong Number 10 structural zone, which indicates that the Tazhong Number I slope belt is more active than its counterpart structural belt and generates oils with more complex geochemical characteristics. The positive correlation between the toluene/methyl cyclohexane ratio and the dibenzothiophene/phenanthrene ratio, as well as with the naphthalene/phenanthrene ratio indicates that aromatization parameters can be used to evaluate the maturity of light crude oils, and there may be inherited relationships between toluene and methyl cyclohexane in crude oils.

Keywords

Aromatic compounds, light crude oils, high maturity, stable carbon/hydrogen isotope, Tarim Basin

[1]State Key Laboratory of Organic Geochemistry, Guangzhou Institute of Geochemistry, Guangzhou, China
[2]University of Chinese Academy of Sciences, Beijing, China
[3]Faculty of Resource, China University of Geosciences, Wuhan, China
[4]Research Institute of Petroleum Exploration & Development, Korla, China

Corresponding author:
Zewen Liao, Kehua Street 511, Tianhe District, Guangzhou 510640, China.
Email: liaozw@gig.ac.cn

Introduction

The Tarim Basin has experienced a number of structural movements, which has led to a series of complex and diverse structural styles, and consequently large differences in oil characteristics between different zones. The fact that large volumes of light crude oil have been extracted from the Tazhong (TZ) area within the Tarim Basin highlights the great potential for massive petroleum exploration from deep layers in this region (He et al., 2016; Wang et al., 2014). Zhu et al. (2015) reported the newly discovered Rewapu oilfield in Tarim Basin, which was well preserved due to low geothermal stress and quick deep burial. Wang et al. (2015) analyzed sulfur-containing compounds in Ha9 and ZS1C crude oils, identifying DBT (dibenzothiophene) series compounds in Ha9 crude oil and thiadiamondoids with 1–3 cages in ZS1C crude oil. Zhang et al. (2015a) conducted a series of geochemical analysis on oil reservoir fluids, suggesting that thermal cracking and TSR have contributed a lot to the deep formation oil. However, because of the high maturity of light crude oils, a number of normal geochemical evaluation parameters cannot be applied. In addition, several structural movements have changed, or even destroyed, crude oils within the Tarim Basin to different degrees; the geothermal changes induced by these movements have affected the thermal evolution of hydrocarbon source rocks and caused large differences in the maturity of crude oils at different phases.

Two sets of source rocks from the CambrianLower Ordovician and Middleto-Upper Ordovician mainly contributed to the oils from Tarim Basin (Zhang and Huang, 2005; Hu et al., 2016; Huang et al., 2017), but the problem which one is the main source have been debated for a few of years (Huang et al., 2016). While some workers believe the main source of hydrocarbons is Middle-to-Upper Ordovician rocks (Hanson et al., 2000; Zhang et al., 2000; Zhao et al., 2005), others have argued that the Cambrian-Lower Ordovician is the main source (Liang et al., 2000; Sun et al., 2003). As this debate remains unresolved, the main aim of this work is to provide a geochemical characterization and discussion of the usage of aromatic compounds in the TZ area rather than to discuss the main source of hydrocarbons within the Tarim Basin.

Compared with other molecules, aromatic hydrocarbons with higher thermal stability are an important research object as their highly delocalized electronic conjugated system makes their energy system low (Xing et al., 2005). This is important because deep layer source rocks in the Tarim Basin are in high mature; source rocks from Cambrian and lower Ordovician strata are considered over mature, and most of these rocks from the middle-to-upper Ordovician fall within the peak oil generation and later oil windows. One good example is the TC 1 well; the equivalent vitrinite reflectance of this well between 5713m and 7124m depth within Ordovician layers is between 1.29% and 2.25% (Zhang et al., 2004), which means that most normal geochemical parameters are invalid because of high maturity (Liang and Chen, 2005). Therefore, this work also discusses the rules governing changes in aromatic hydrocarbons within TZ crude oils.

Light hydrocarbon is another series of compounds for petroleum research. Liu et al. (2015) reported the light composition, hydrogen and carbon isotope of the upper Paleozoic gases in the Ordos Basin and suggested that they were all sourced from Carboniferous–Permian coal-bed source rocks, distinguishing two type of natural gas. Han et al. (2017) used MCH (methyl cyclohexane) index to identify Upper Paleozoic

gas source rocks in Shenmu gas field and think they are mainly of humic genesis of swamp facies.

Samples and methods

Samples

A total of 89 oils samples were selected for analysis in this work from the TZ Number I fault zone, the TZ Number 10 structural zone, and the central uplift zone. These samples comprise 49 black oils and 40 light crude oils, collected from different districts of TZ area. The black oils are mainly from depths between 3000 m and 5000 m, while light crude oils mainly from depths between 5000 m and 6500 m. The distribution of oil samples is shown in Figure 1.

Methods

The samples were treated by following steps.

(1) About 3 mg of the TZ black oils were taken and separated into saturates and aromatics by successively using hexane and a mixture solvents (hexane: dichloromethane = 1:3) in a 9 cm column filled with 3:1 silica gel and aluminum oxide.
(2) All separated components were analyzed with a Thermo TRACE GC Ultra combined to a DSQ II mass instrument which was fitted with a HP-5 mass spectrometry (MS) capillary column (30 m × 0.32 mm × 0.25 μm). Helium was used as the carrier gas at a current speed of 1.2 mL/min, and the injection temperature was set at 295°C. The heating procedure for saturates is set as 80°C for 4 min, followed by heating of 4°C/min up to

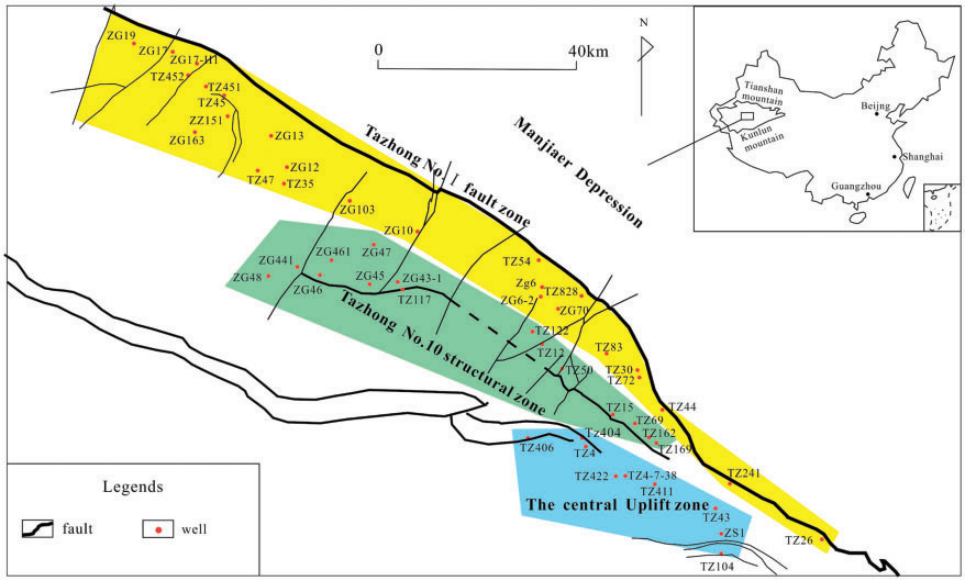

Figure 1. Tectonic units that comprise the Tazhong Uplift and locations of the oil samples discussed in this work.

295°C, and then held for 20 min. The heating procedure for aromatics as 80°C for 4 min, followed by heating of 3°C/min up to 295°C, then held for 20 min.

(3) The light crude oils were directly used for the analyses without separation, and then the heating procedure is set as 35°C held steady for 4 min, followed by heating at a rate of 4°C/min up to 295°C, and then held for 30 min.

(4) TZ light crude oils were analyzed using a GV isoprime GC–MS to determine the specific stable carbon (C) and hydrogen (H) isotope values of their toluene and methyl cyclohexane compounds. Thus, compounds specific C isotope values were analyzed using a GV isoprime GC–MS fitted with a capillary column HP-1MS (30 m × 0.25 mm × 0.25 μm). Finally, compound specific C isotope values were analyzed using a ThermoFisher gas chromatography GC-IRMS fitted with a HP-1MS capillary column (30 m × 0.25 mm × 0.25 μm). The heating procedure and carrier gas are the same as previously described for GC–MS.

Results and discussion

The geochemical analysis results of the black oils and light crude oils are presented in Tables 1 and 2, respectively.

Distribution characteristics of saturates and aromatics in TZ black oils

A total ion chromatogram (TIC) and the compounds identified in selected TZ black oil samples are presented in Figure 2; within these samples, TZ26, TZ44 and TZ241 are located within the TZ Number I fault zone, while TZ4, TZ104 and TZ404 are located within TZ Number 10 structural zone, and TZ12, TZ35 and TZ162 are located within the central uplift zone.

The distribution of *n*-alkanes showed that TZ black oils mainly ranges between C_{13} and C_{30}, with the main peak between C_{15} and C_{16}. The pristane (Pr)/phytane (Ph) ratio falls between 0.83 and 1.32; this ratio for samples from TZ Number 10 structural zone mainly ranges between 0.80 and 1.00, while mainly ranges between 1.00 and 1.20 for samples from TZ Number I fault zone. The UCM (Unidentified Complex Mixture) peaks in some samples suggested their suffering from biodegrading, which means that these TZ oil reservoirs may have experienced more than once charges. And it seems that the early charged oils were biodegraded before being mixed with the later charged oils.

Table 1 lists the biomarker parameters of tricyclic terpanes, hopanes, steranes, and gammaceranes. These data show that the gammacerane/C_{30} αβ hopane ratio for oils from the TZ Number 10 structural zone as well as the central uplift zone mostly range between 0.05 and 0.31, while samples from the TZ Number I fault zone mainly range between 0.08 and 0.21. Data also reveal a low abundance of tricyclic terpanes as well as a relatively high abundance of pentacyclic terpanes; the C_{23}/C_{21} tricyclic terpane ratio ranges between 1.05 and 2.42, while that of C_{29}/C_{30} hopanes ranges between 0.42 and 1.39. The distribution of steranes in these samples is C_{27} regular steranes between 19.00% and 50.14%, while C_{28} steranes occur between 16.66% and 37.63% abundance, and C_{29} steranes occur between 33.13% and 55.58%, which is generally characterized by an overall ratio relationship $C_{27} > C_{28} < C_{29}$. At the same time, however, a few sterane parameters of these samples display the ratio $C_{27} < C_{28} < C_{29}$. These results indicate hydrocarbon precursors derived from bacteria

Table 1. Geochemical parameters of Tazhong black oils.

Zone	Well	Depth (m)	Strata	pr/ph	G/C_{30} H	C_{23}/C_{21} TT	C_{29}/C_{30} H	C_{27} (%)	C_{28} (%)	C_{29} (%)	4-/1-MDBT	4-MDBT/DBT	Ro (MDR)	DBT/P	MPI1	MPI2	Ro (MPI)
Tazhong No. 1 fault zone	tz241	4618.47–4725.74	O	1.20	0.05	1.21	0.74	50.14	16.66	33.19	6.42	1.47	1.40	0.26	0.68	0.74	0.81
	tz242	4065.15	S	0.92	/	1.42	0.64	35.07	13.46	51.47	4.91	0.62	1.33	1.71	0.68	0.78	0.81
	tz26	4300–4315	O	1.08	0.08	1.51	0.72	23.28	25.86	50.86	4.93	1.37	1.33	0.62	0.65	0.74	0.79
	tz26	4335–4360	O1	1.04	0.17	1.43	0.65	10.43	26.25	63.32	4.46	1.18	1.30	0.45	0.60	0.67	0.76
	tz30	4997–5026	O	1.10	0.31	1.58	0.42	19.00	32.13	48.87	6.22	1.44	1.39	0.49	0.55	0.62	0.73
	tz30	4244.5–4260	S	1.23	0.19	1.47	0.56	27.96	26.28	45.76	2.22	1.49	1.12	0.43	0.73	0.90	0.84
	tz44	4854–4888.31	C2+3	0.97	0.07	1.94	1.01	21.76	34.84	43.40	6.04	1.34	1.38	0.75	0.57	0.60	0.74
	tz44	4822.00	O1+2	1.12	0.15	1.50	0.74	19.79	34.50	45.70	5.19	1.36	1.34	1.06	0.66	0.76	0.80
	tz45	6020–6150	O1	0.97	/	1.77	1.39	41.33	23.58	35.09	6.14	1.62	1.39	1.24	0.63	0.75	0.78
	tz451	6050–6297.62	O1+2	0.97	/	1.92	0.98	41.85	25.01	33.15	6.92	1.80	1.42	1.52	0.67	0.77	0.80
	tz452	6376.76–6550	O1+2	1.04	0.25	1.62	0.54	21.09	36.70	42.22	4.64	1.64	1.31	0.23	0.42	0.47	0.65
	tz54	5832–5858	O	0.94	0.13	1.66	0.52	30.22	31.30	38.48	13.12	3.58	1.59	0.30	0.66	0.72	0.80
	tz62	4700.5–4758	O	1.03	0.04	1.59	0.66	12.76	29.99	57.25	9.12	1.38	1.49	0.89	0.81	0.91	0.89
	tz622	4913.52–4925	O	0.94	0.08	1.93	0.67	32.61	15.46	51.94	5.19	1.51	1.34	2.07	0.66	0.73	0.80
	tz72	4964–4978	O	1.11	0.10	1.53	0.53	33.55	24.70	41.75	8.64	1.66	1.48	0.60	0.64	0.73	0.78
	tz72	5125–5130	O	1.04	/	1.81	0.65	48.30	18.56	33.13	1.93	1.31	1.08	2.08	0.46	0.51	0.68
	tz83	5433–5441	O	1.06	0.02	1.62	0.62	44.54	21.00	34.47	8.89	1.65	1.49	0.67	0.75	0.85	0.85
	tz824	5744.59–5750	O	0.87	0.06	1.40	0.54	19.78	30.36	49.87	24.66	2.82	1.76	0.37	0.75	0.84	0.85
	tz828	5595–5603	O	1.04	0.13	1.57	0.45	33.25	29.03	37.72	7.43	2.84	1.44	0.26	0.66	0.71	0.80
Tazhong No.10 structural zone	tz117	4422.57–4436.12	S	0.89	0.06	1.97	0.88	20.56	18.64	60.80	3.61	1.08	1.25	1.62	0.66	0.84	0.80
	tz117	4450–4453	S	0.94	0.06	1.90	0.85	21.67	17.33	60.99	4.81	1.10	1.32	1.15	0.66	0.81	0.79
	tz12	4631.88–4733.92	O	0.83	0.03	2.01	0.75	34.55	21.77	43.68	5.87	1.84	1.37	0.42	0.71	0.83	0.83
	tz12	4695.5–4777.5	O	0.91	0.07	1.79	0.70	26.95	21.36	51.69	4.68	1.67	1.31	0.43	0.78	0.92	0.87
	tz12	4374.5–4413.5	S	0.94	0.09	1.91	0.71	26.79	22.18	51.03	3.01	1.29	1.20	0.78	0.84	1.05	0.90
	tz122	4707.88–4733.92	O	0.96	0.03	2.42	0.78	36.14	21.83	42.03	5.98	1.71	1.38	0.44	0.66	0.78	0.80
	tz122	4333.8–4344.4	S	1.02	0.08	2.20	0.76	27.56	21.62	50.83	3.28	1.48	1.22	0.63	0.82	0.98	0.89
	tz122	4349–4352.7	S	0.98	0.08	1.88	0.72	32.30	22.94	44.76	5.79	1.97	1.37	0.80	0.78	0.89	0.87
	tz15	4300–4306.5	S	0.89	0.11	1.74	0.76	35.24	26.41	38.36	2.12	1.48	1.10	0.42	1.12	1.60	1.07
	tz161	4178–4181	S	0.99	0.08	1.73	0.72	29.34	18.76	51.90	4.44	0.98	1.30	1.34	0.66	0.75	0.80
	tz162	3840–3842.5	C	0.98	0.28	1.22	0.54	33.69	26.21	40.10	3.39	1.28	1.23	1.18	0.86	1.03	0.91
	tz169	4241.09–4283.52	O	0.94	0.06	2.02	0.79	33.94	20.94	45.12	5.12	2.22	1.34	0.63	0.73	0.82	0.84
	tz169	4119.56–4149.16	S	1.32	0.10	1.72	0.59	42.45	22.85	34.70	2.10	1.35	1.10	0.40	0.83	0.99	0.90

(continued)

Table 1. Continued

Zone	Well	Depth (m)	Strata	pr/ph	G/C_{30} H	C_{23}/C_{21} TT	C_{29}/C_{30} H	C_{27} (%)	C_{28} (%)	C_{29} (%)	4-/1-MDBT	4-MDBT/DBT	Ro (MDR)	DBT/P	MPI1	MPI2	Ro (MPI)
the central uplift zone	tz35	4269.68–4333.92	C3	0.99	0.07	1.84	0.64	30.97	28.85	40.18	3.90	3.66	1.27	0.28	1.22	1.36	1.13
	tz35	4946–4951	S	0.97	0.03	1.73	0.76	25.59	24.33	50.09	3.21	1.47	1.21	0.50	0.72	0.83	0.83
	tz40	4334–4340	C3	0.89	0.13	2.06	0.86	21.72	22.68	55.60	4.89	1.29	1.33	1.97	0.76	0.91	0.86
	tz47	4978.5–4986	S	1.03	0.10	1.79	0.83	24.13	17.85	58.02	6.22	1.66	1.39	1.25	0.85	0.98	0.91
	tz50	4378.5–4385	S	0.88	0.08	1.60	0.75	33.15	18.99	47.86	5.22	2.05	1.34	0.32	0.68	0.80	0.81
	tz69	4368.5–4377	S	1.02	/	1.05	0.99	37.91	23.96	38.13	3.50	1.68	1.24	0.37	0.74	0.88	0.84
	tz104	3647–3669	C2	1.22	0.05	2.01	0.86	26.85	20.97	52.18	7.22	1.69	1.43	1.17	0.74	0.81	0.84
	tz4	3532–3548	C3	0.99	0.06	2.10	0.98	21.20	37.63	41.18	6.91	1.94	1.42	1.73	0.78	0.83	0.87
	tz404	3619.47–3681.81	C	1.01	0.11	2.16	0.82	31.46	20.94	47.60	6.49	1.84	1.40	2.20	0.83	0.90	0.90
	tz406	3646.92–3692.26	C	0.90	0.21	0.81	0.79	25.94	18.82	55.23	4.37	1.62	1.30	0.71	0.55	0.69	0.73
	tz406	3646.92–3692.27	C	0.88	0.22	2.12	0.91	36.00	18.47	45.53	5.87	1.96	1.37	0.84	0.68	0.76	0.81
	tz406	3952.5–4128.63	C3	0.99	0.10	2.09	0.82	24.64	14.78	60.58	5.89	1.59	1.38	1.79	0.73	0.82	0.84
	tz411	3263–3450	C	0.96	0.08	2.12	1.01	28.83	20.82	50.36	5.38	2.49	1.35	1.66	0.81	0.91	0.89
	tz422	3537–3554	C1	0.99	0.06	2.03	1.34	26.47	17.94	55.58	5.67	1.89	1.37	1.11	0.74	0.79	0.84
	tz43	3652–3554	O	1.01	0.15	1.30	0.65	42.01	8.47	49.52	13.22	1.75	1.59	0.91	0.78	0.88	0.87
	tz4-7-38-1	3936.43–3985.5	O	0.92	0.10	1.69	1.10	30.54	18.74	50.73	2.74	1.28	1.17	0.75	0.78	0.91	0.87
	tz52	3808.46–3831.5	O	1.20	0.04	1.22	0.79	20.44	18.40	61.16	10.53	1.94	1.53	1.21	0.86	0.98	0.91

G/C_{30} H: gammacerane/C_{30} hopane; C_{23}/C_{21} TT: C_{23} tricyclic terpane/C_{21} tricyclic terpane; C_{29}/C_{30} H: C_{29} hopane/C_{30} hopane; C_{27} (%), C_{28} (%), and C_{29} (%) refer to C_{27}, C_{28}, and C_{29} steranes; MDBT: methyldibenzothiophene; DBT: dibenzothiophene; MDR = 4-/1-MDBT; MPI1: methylphenanthrene indicator 1; MPI2: methylphenanthrene indicator 2.

Table 2. Geochemical parameters of Tazhong light crude oils.

Zone	Well	Depth (m)	Strata	Tol/ MCH	2-/ 1-MN	MN/ DMN	DMN/ TMN	N/P	DBT/P	4-MDBT/ DBT	4-/1- MDBT	Ro (MDR)	MPI1	MPI2	Ro (MPI)
Tazhong No. 1 fault zone	ZG10	6198–6309	O	1.61	1.68	1.13	2.24	8.86	2.55	1.10	4.59	1.31	0.80	0.93	0.88
	ZG101	6998–6309		1.16	2.24	0.77	1.18	4.84	2.04	1.29	2.06	1.10	1.06	1.21	1.03
	ZG102	6022.5–6410		1.77	2.73	0.80	3.26	9.04	5.84	0.80	5.88	1.38	0.74	0.76	0.84
	ZG103	6105–6223		1.19	1.51	0.59	1.33	7.44	0.64	1.24	6.23	1.39	0.72	0.84	0.83
	ZG105	5936–6829.28	O1y	1.37	1.98	0.51	0.90	5.04	4.47	0.97	2.81	1.18	0.72	0.79	0.83
	ZG106	6110–6115		1.40	2.48	0.69	1.66	15.21	3.54	4.20	6.73	1.41	0.86	0.92	0.92
	ZG11-7H	6263–6302.7	O	1.16	2.81	0.88	1.61	30.14	3.37	3.42	3.02	1.20	0.79	0.88	0.87
	ZG12	6059.58–6279	O	1.60	1.67	0.84	1.73	6.90	1.71	1.40	10.84	1.54	0.54	0.64	0.72
	ZG13	6458–6550.36	O3L	1.35	1.43	0.54	1.25	4.63	2.81	1.52	5.84	1.37	0.57	0.75	0.74
	ZG13-1H	5886–7135		0.93	1.93	0.65	1.03	3.18	1.09	1.62	5.88	1.38	0.80	0.89	0.88
	ZG14-1	6133–6298	O	2.01	2.08	0.77	1.54	10.56	3.52	1.16	5.16	1.34	0.78	0.82	0.87
	ZG151	6083.75–6223.81	O2	1.84	1.64	0.69	1.44	15.98	2.20	1.08	4.91	1.33	0.50	0.59	0.70
	ZG162-H2	6104.05–7495	O	1.36	1.43	1.04	2.36	30.25	1.90	1.55	3.69	1.25	0.67	0.60	0.80
	ZG163	6140–6224		0.98	1.48	0.64	0.91	6.63	2.09	1.62	6.14	1.39	0.58	0.71	0.75
	ZG164	6122.13–6213.58	O	1.34	1.91	0.58	1.14	5.53	2.39	1.44	5.45	1.36	0.51	0.56	0.70
	ZG17	6206–6446	O1y	1.16	1.81	0.82	1.51	10.08	4.33	0.60	3.72	1.25	0.67	0.77	0.80
	ZG17-H1	6088–6887		1.01	1.21	1.14	2.32	6.36	1.01	1.42	4.59	1.31	0.54	0.64	0.73
	ZG19	6381–6438.5	O	0.63	1.23	0.63	1.22	3.63	0.64	1.80	6.54	1.40	0.73	0.79	0.84
	ZG21-H	5995–6060	O	1.46	1.81	0.79	1.00	9.06	2.36	0.82	3.10	1.20	0.66	0.66	0.80
	ZG22	5605–5736.66	O	1.55	1.79	0.59	1.13	5.06	1.82	1.49	6.62	1.41	0.71	0.79	0.83
	ZG501	6515.5–6790.4		1.17	1.87	0.52	1.21	3.68	4.19	1.48	9.55	1.50	0.54	0.62	0.72
	ZG503	5919–6100		1.67	1.50	0.51	1.14	6.00	3.37	1.49	4.61	1.31	0.79	0.91	0.87
	ZG6	5934.5–6172.73	O1y	2.37	1.49	0.63	1.30	13.52	6.23	0.91	3.65	1.25	0.67	0.81	0.80
	ZG6-2	5898.25–6143.17	O1y	2.12	1.63	0.59	1.53	10.16	5.50	1.21	4.31	1.29	0.72	0.84	0.83
	ZG7	5865–5885		1.73	2.53	0.79	1.78	3.88	4.40	1.40	3.86	1.26	0.64	0.85	0.78
	ZG70	5714–5728		1.32	1.31	0.68	0.95	9.22	4.54	0.97	2.86	1.18	0.68	0.85	0.81
	ZG702	5628–5890	O	2.21	2.02	0.85	1.69	12.59	9.64	0.91	5.49	1.36	0.61	0.74	0.76

(continued)

Table 2. Continued

Zone	Well	Depth (m)	Strata	Tol/ MCH	2-/ 1-MN	MN/ DMN	DMN/ TMN	N/P	DBT/P	4-MDBT/ DBT	4-/1- MDBT	Ro (MDR)	MPI1	MPI2	Ro (MPI)
Tazhong No.10 structural zone	ZG43-1	5200–5348	O1H	1.30	1.78	0.71	1.44	5.98	2.67	1.21	9.65	1.51	0.60	0.70	0.76
	ZG43-1	5200–5798	O1y	1.17	1.37	0.70	0.87	6.48	2.05	1.18	4.06	1.28	0.66	0.77	0.79
	ZG441	5414.38–5522		1.21	1.57	0.68	1.10	4.08	1.38	0.92	5.23	1.34	0.59	0.69	0.75
	ZG44C	5432–5861.50		1.27	2.03	0.62	1.21	7.77	3.06	1.13	4.87	1.33	0.74	0.78	0.84
	ZG45	5637.2–5650.17	O3	1.19	1.36	0.65	1.08	2.92	1.85	1.12	4.24	1.29	0.65	0.77	0.79
	ZG46	5039.40–5367.34	O3	3.03	1.52	0.70	1.44	14.71	3.91	1.37	4.43	1.30	0.83	0.95	0.90
	ZG461	5479.64–5745		1.04	1.42	0.75	1.23	4.63	1.49	1.26	4.83	1.32	0.63	0.65	0.78
	ZG461	5479.64–5740		1.07	1.71	0.67	1.41	4.94	1.58	1.24	5.77	1.37	0.60	0.71	0.76
	ZG462	5431–5981		1.16	1.63	0.49	0.85	2.48	3.25	1.08	2.86	1.18	0.82	0.86	0.89
	ZG47	5811–6095		0.79	1.51	0.66	0.83	8.13	0.86	2.14	6.20	1.39	0.65	0.74	0.79
	ZG47CH	6489–6606		0.80	1.92	0.59	1.19	4.71	0.87	2.03	6.22	1.39	0.74	0.81	0.84
	ZG48	5498.1–5531.54		0.86	1.26	1.15	2.18	3.51	0.80	0.80	3.65	1.25	0.54	0.62	0.73
	ZS1	6426–6497	$\in$	1.10	2.18	1.30	2.35	2.89	0.24	2.26	5.67	1.37	1.18	1.35	1.11

Abbreviations (in addition to those already listed in the text and below Table 1): Tol: toluene; MCH: methyl cyclohexane; MN: methylnaphthalene; DMN: dimethylnaphthalene; TMN: trimethylnaphthalene; N: naphthalene; P: phenanthrene.

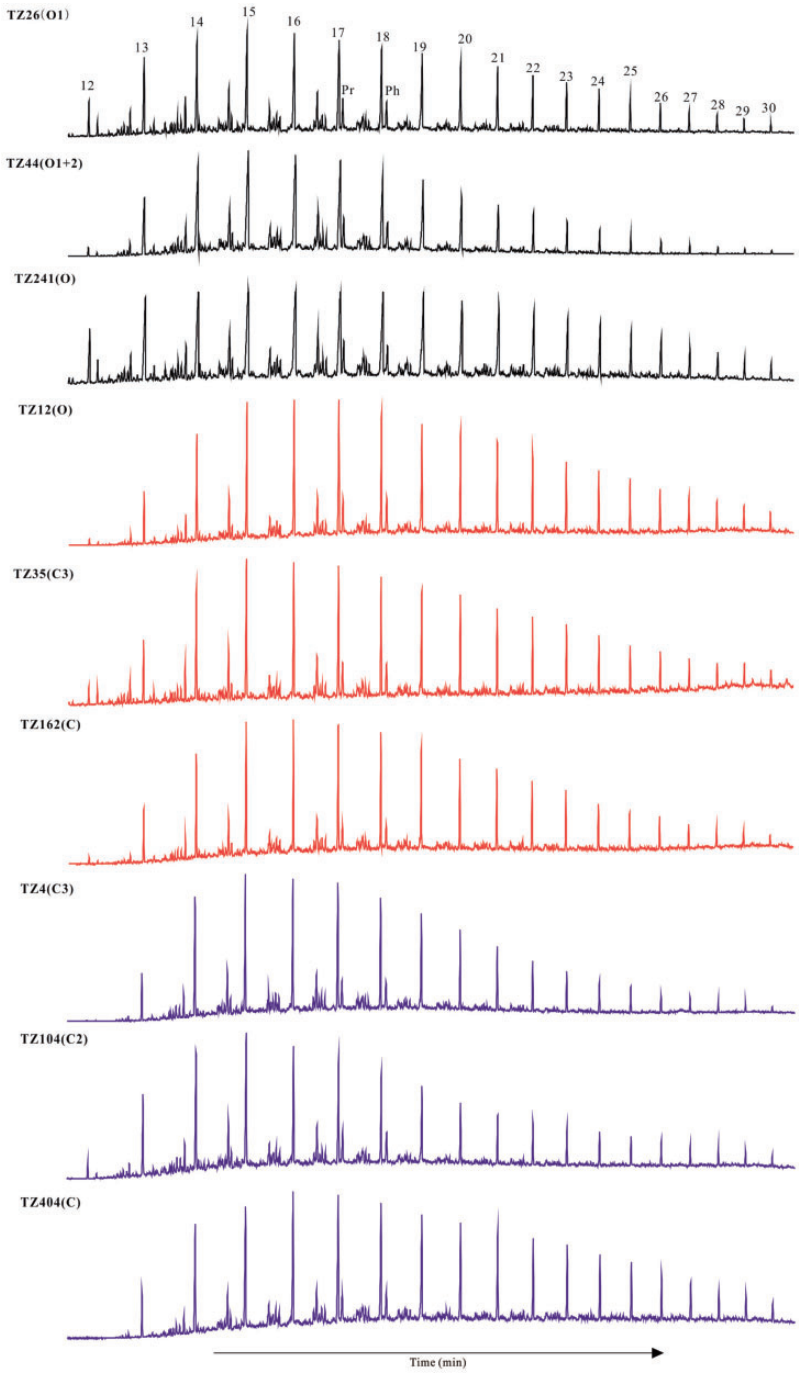

Figure 2. Selected TICs of some Tazhong black oil samples. Wells TZ26, TZ44 and TZ241 are located within the Tazhong Number I fault zone, while TZ4, TZ104 and TZ404 are located within the Tazhong Number 10 structural zone, and TZ12, TZ35 and TZ162 are located within the central uplift zone. The numbers above peaks denote *n*-alkane carbon numbers.

TIC: total ion chromatogram.

and seaweed, while differences in sterane distribution might be the result of several charging phases.

Results (Table 1) show little difference between the oil samples from different structural zones concerning the distribution of regular biomarker parameters because these parameters have been homogenized by the facts that the oil generating rocks within the Tarim Basin comprise several sources (Jin, 2005; Yun et al., 2014), which have experienced several charging phases (Chang et al., 2013; Zhao et al., 2012) and characterized by the adjustment and destruction of generated hydrocarbons (Zhuo and Wang, 1999). Thus, three tectonic phases can be identified corresponding with the end of the Early Paleozoic, the Late Paleozoic-to-Early Mesozoic, and the Late Cenozoic; these match with the oil charging phases of the Tarim Basin, specifically named as the late Caledonian-to-Hercynian, the late Hercynian and Himalayan periods (Zhang et al., 2011). Oils from the Cambrian source rocks (late Caledonian-to-Hercynian) have generally been destroyed, which is accordant to that the Late Hercynian is the main oil reserved period of the two source rocks. The Himalayan period was the main time for gas generation, as gas invading condensate gas reservoirs formed during this period (Zhang et al., 2012). In contrast, samples containing crude oils from these three generating phases also have particular characteristics as they formed in distinct structural zones, all of which were highly saline marine facies derived from bacterial and seaweed precursors.

The aromatic hydrocarbon components of samples mainly comprise naphthalene and alkylnaphthalene, as well as phenanthrene and alkylphenanthrene, fluorene and alkylfluorene, and dibenzothiophenes, particularly among which the naphthalene and phenanthrene homologues occur at higher abundances. Earlier work concerning methylphenanthrene parameters have been related to maturity (Radke et al., 1982). Indeed, both the methylphenanthrene indicator 1 (MPI1) and methylphenanthrene indicator 2 (MPI2) values of source rocks initially increase and then decrease as depth increases; calculated MPI1 values [MPI = $1.5 \times$ (2-methylphenanthrene + 3-methylphenanthrene)/(phenanthrene + 1-methylphenanthrene + 9-methylphenanthrene)] for TZ black oils range between 0.42 (TZ452) and 1.22 (TZ35) (although mainly concentrated between 0.55 and 0.85), while MPI2 values [MPI2 = $3 \times$ (2-methylphenanthrene)/(phenanthrene + 1-methylphenanthrene + 9-methylphenanthrene)] of these samples range between 0.47 (TZ452) and 1.36 (TZ35) (mainly between 0.69 and 0.91). Equivalent vitrinite reflectances (Ro%) calculated based on MPI (Ro% = $0.60 \times$ MPI1 + 0.40) (i.e. $0.65 \leq$ Ro% < 1.35) range between 0.73 and 1.13.TZ oils derived from marine source rock while MPI mainly works for type III kerogen, thus calculated Ro cannot well correlate to source rock and then less reliable.

In terms of sulfur-containing aromatic compounds, it is informative of different locations of methyl groups within methyldibenzothiophenes as they are indicative of thermal stability (4-MDBT > 1-MDBT). Research in this area was performed by Dzou et al. (1995) who reported that the relationship between MDR (4-MDBT/1-MDBT) and equivalent vitrinite reflectance is Ro% = $0.2663 \times$ Ln (MDR) + 0.9034. Compounds of this type have been studied in details (Chakhmakhchev et al., 1997; Luo et al., 2001; Santamaría-Orozco et al., 1998). Zhou et al. (2008), for example, calculated the maturity of source rocks at different depths within the TC1 well using this formula. The MDR of oil samples ranged between 1.93 and 24.66, while MDR4 (4-MDBT/DBT) ranged between 0.62 and 3.66, and Ro% ranged between 1.08 and 1.76, which is more reliable than the Ro calculated by MPI. At the same time, it is also noteworthy that, in addition to maturity,

aromatic sulfur-containing compound parameters may also be influenced by other factors including biodegradation.

Geochemical characterization of Tazhong light crude oils

Overall geochemical properties of the light crude oils. Some TIC results of TZ light crude oils are illustrated in Figure 3, among which ZG10, ZG70 and ZG12 are located within the TZ

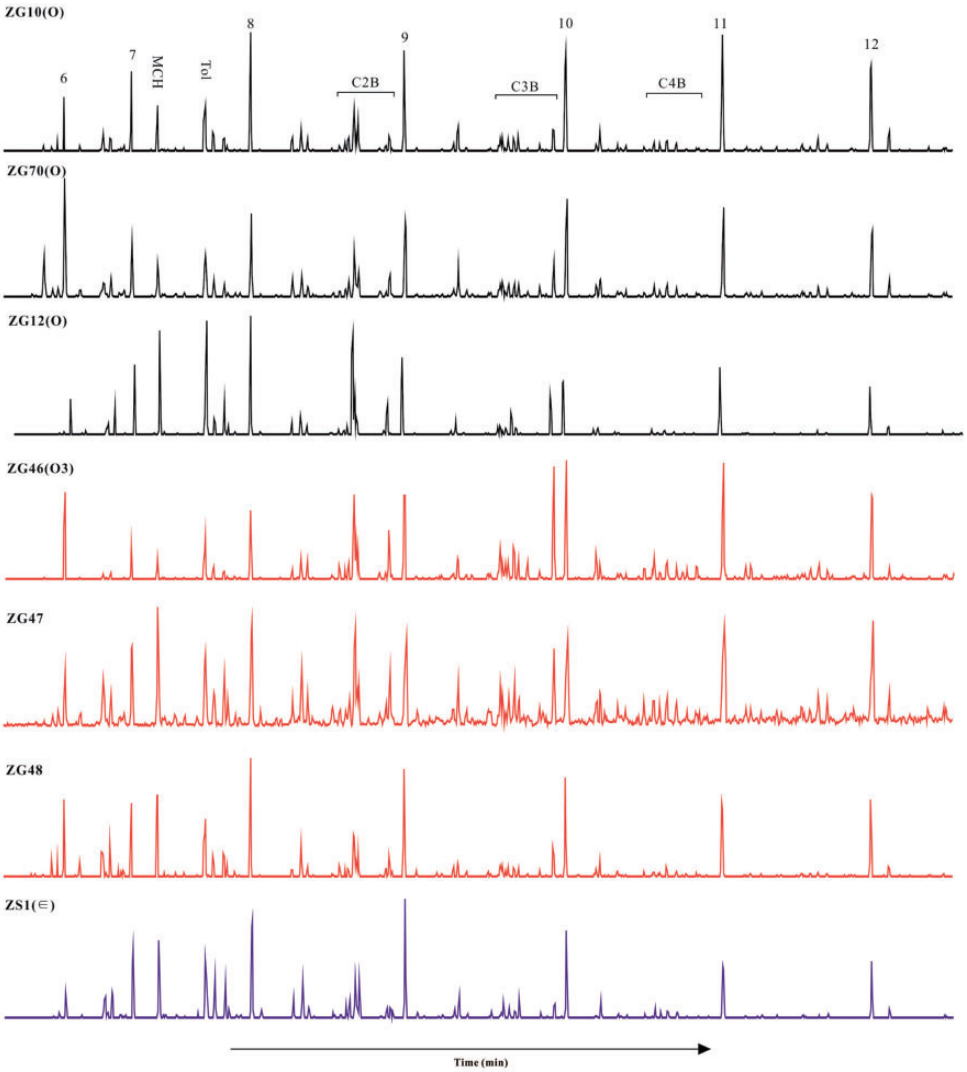

Figure 3. Partial TICs of selected light crude oil samples. Numbers above peaks represent *n*-alkane carbon numbers.

TIC: total ion chromatogram; C2B: C_2 substituted benzene; C3B: C_3 substituted benzene; C4B: C_4 substituted benzene.

Number I fault zone, while ZG46, ZG47 and ZG48 are located within the TZ Number 10 structural zone, and the ZS1 reservoir is located in the central uplift zone deposited in Cambrian strata. As these samples mainly belong to light crude oils, the *n*-alkanes in samples are light hydrocarbons with low carbon number. As an example, the sample from well ZG12 has a peak *n*-alkane at C_8 which demonstrates high maturity; this also means that most normally detected biomarkers are not present and so the regular geochemical parameters usually applied to sample characterization are also invalid. Rich aromatic hydrocarbons are detectable in all these samples including alkylbenzene, alkylnaphthalene and alkylphenanthrene as well as biphenyl, alkyldibenzothiophene.

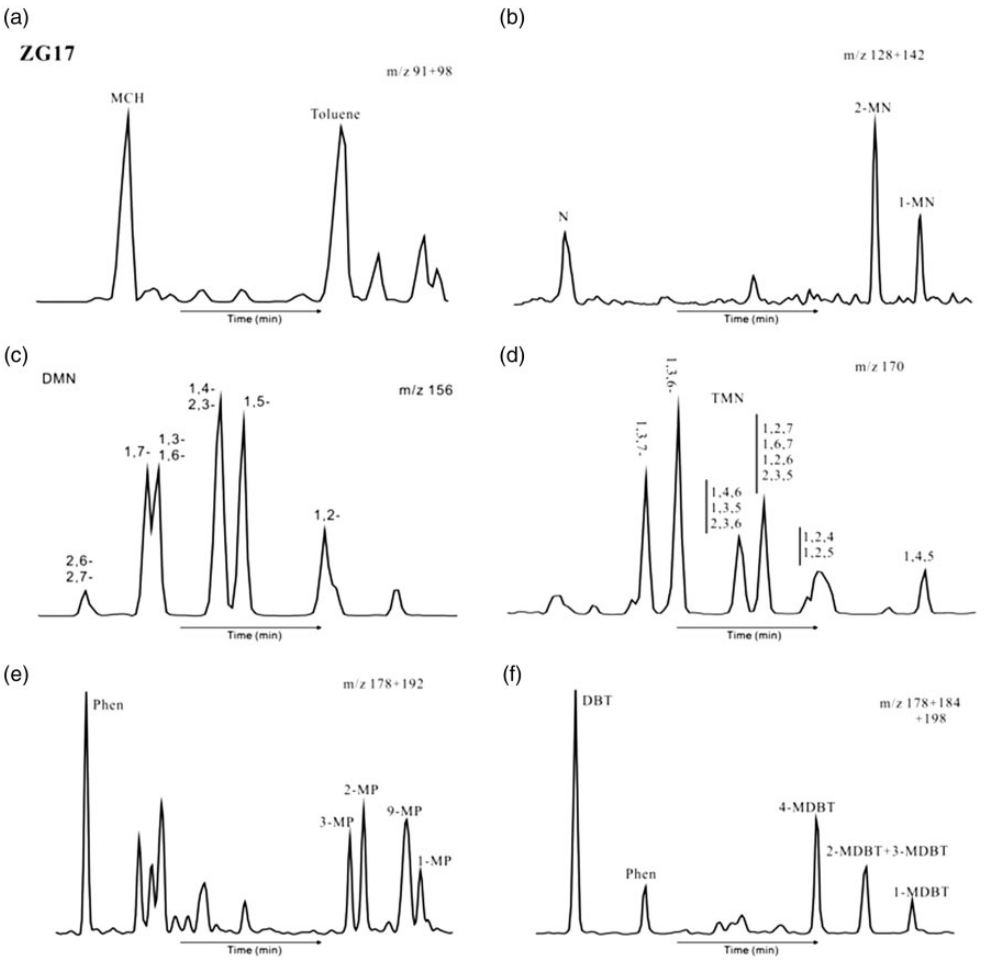

Figure 4. Partial mass chromatograms of light crude oils from ZG17.

MCH: methylcyclohexane; N: naphthalene; MN: methylnaphthalene; DMN: C_2 substituted naphthalene; TMN: C_3 substituted naphthalene; Phen: phenanthrene; MP: methylphenanthrene; DBT: dibenzothiophene; MDBT: methyldibenzothiophene.

For ZG17 light crude oil, the mass chromatograms exemplified by ions of m/z 91, 98, 128, 142, 156, 170, 178, 184, 192 and 198 are presented in Figure 4. Toluene and methylcyclohexane in the samples may share some common geochemical origin as they may have been derived from the same precursor molecules and even the toluene may be derived from methylcyclohexane in the oil reservoirs, and then the ratio of toluene to methyl cyclohexane will be further discussed concerning their geochemical characteristics including maturity.

Geochemical characteristics of the aromatics of the light crude oils. Some geochemical parameters of aromatic compounds in TZ light crude oils are shown in Figure 5. In terms of the first group, the ratio between toluene and methyl cyclohexane ranges between 0.63 and 3.03 (mainly between 0.98 and 2.01). The ratio between these compounds in samples from the TZ Number I fault zone ranges more widely than those for the TZ Number 10 structural zone, with ratios for the latter concentrated between 0.79 and 1.30, however with the exception for ZG46 sample (also see the following discussion).

Some previous research has suggested that a high abundance of naphthalene series compounds is indicative of highly mature source rocks (Price, 1993). In TZ45 condensate oils and light crude oils, the abundance of naphthalene series is relatively high (Zhou et al., 2008). Similarly, in terms of methylnaphthalene (MN) molecular characteristics, methyl in location β tend to be more stable than those in location α, which means that 2-MN tend to exhibit higher thermal stability than their 1-MN counterparts. Thus, the ratio between 2-MN and 1-MN compounds can be applied for maturity comparisons of light crude oils.

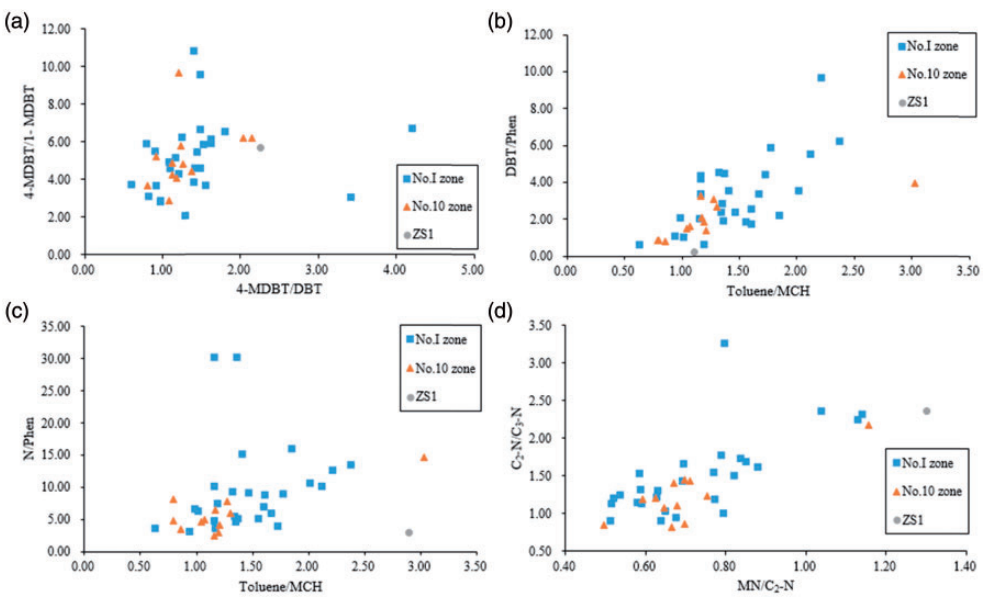

Figure 5. Cross-plots for Tazhong light crude oils: (A) 4-MDBT/1-MDBT ratios versus 4-MDBT/DBT ratios; (B) toluene/MCH ratios versus DBT/phenanthrene ratios; (C) naphthalene/phenanthrene ratios versus toluene/MCH ratios; and (D) DMN/TMN ratios versus MN/DMN ratios.

MDBT: methyldibenzothiophene; DBT: dibenzothiophene; MCH: methylcyclohexane; DMN: C_2 substituted naphthalene; TMN: C_3 substituted naphthalene; MN: methylnaphthalene.

Our results show that the MN indicators (2-MN/1-MN) in TZ light crude oils range between 1.21 and 2.81. Comparing these results with research on MN compounds from Li and Wang (2005) suggests that the Ro% of samples should be more than 1.0%; however, this previous result was based on low maturity samples and so a difference should be expected when compared to the high maturity oils discussed in this work. Indeed, in the case of multiple-substituted naphthalene parameters, MN/C_2 substituted naphthalenes (DMN) ratios of our samples range between 0.49 and 1.30; specifically, this ratio for samples from the TZ Number I fault mainly between 0.51 and 0.88 while those from the TZ Number 10 structural zone between 0.59 and 0.75. At the same time, DMN/C_3 substituted naphthalenes (TMN) ratios range between 0.83 and 3.25; this ratio in samples from the TZ Number I fault zone mainly between 0.90 and 1.78, while for samples from the TZ Number 10 structural zone range between 0.83 and 1.44.

Values of MPI were chosen to illustrate the parameters of phenanthrene series compounds. Results show that MPI1 values for light crude oils range between 0.61 and 1.18 while MPI2 values range between 0.56 and 1.35. Thus, equivalent Ro% values calculated using MPI (i.e. $Ro\%_a = 0.60 \times MPI1 + 0.40$; $0.65 \leq Ro\% < 1.35$; $Ro\%_b = -0.60 \times MPI1 + 2.30$; $1.35 \leq Ro\% < 2.00$) range between 0.72% and 1.11% and between 1.59% and 2.00%, respectively. At the same time, the ratios between naphthalene and phenanthrene range between 2.48 and 30.25; results show that N/phenanthrene ratios for samples from the TZ Number I fault zone range between 3.18 and 30.25, a much wider variation than those from the TZ Number 10 structural zone between 2.48 and 8.13 (with the exception for ZG46).

The MDR of oil samples ranged between 2.06 and 10.84, while MDR4 (4-MDBT/DBT) ranged between 0.60 and 4.20, and Ro% ranged between 1.10 and 1.51.

Our results show that the DBT/phenanthrene ratios of TZ oil samples range between 0.24 and 9.6; these ratios in samples from the TZ Number I fault zone are between 0.64 and 9.64, a wider range than samples from the TZ Number 10 structural zone of 0.80 and 3.91 (with the exception for ZG46). Reported by Zhang et al. (2015b), the extremely high DBT/phenanthrene ratios may be influenced by TSR (Thermal Sulfate Reduction). The results of MN/DMN, DMN/TMN, toluene/MCH, DBT/phenanthrene, and naphthalene/phenanthrene ratios of light crude oils from the TZ Number I fault zone range widely, while those from the TZ Number 10 fault zone encompass a relatively narrow range (Figure 5). This result indicates that oil samples from the TZ Number I fault zone have undergone more oil charging than their counterparts; indeed, even oils generated from the same hydrocarbon source rock with the same original material exhibit differences in maturity because they were generated in different hydrocarbon expulsion phases. In other words, the oil samples from the TZ Number I fault zone are more complicated in composition than their counterparts from the TZ Number 10 structural zone, as illustrated by the geochemical parameters discussed in this study.

Qiu et al. (1997, 2010, 2012) and Liu et al. (2017) performed a lot of work in investigating hydrocarbon charge. In earlier work, Qiu et al. (1997, 2010, 2012) analyzed a series of integrated thermal indicators of apatite and zircon (U–Th)/He ages, as well as apatite fission tracks, and equivalent vitrinite reflectance data from TZ source rocks. Their results were used to hypothesize that Indosinian and Yanshan movements lifted strata in this region and made multistage accumulation possible as source beds moved into a detained stage and stopped generating oil and gas following rapid source rock maturation. In a similar study, Yang et al. (2011) performed research on fluid inclusions within a TZ Ordovician carbonate reservoir and suggested three distinct phases of oil charging, namely Caledonian-to-early

Hercynian, late Hercynian, and Himalayan stages. The last phase of the Himalayan, was mainly charged with gas. Thus, as the characteristics of TZ light crude oils were influenced by oil charging during Himalayan gas invading stage, they share similar features with condense oils as the late Hercynian. In contrast, as oil charging during the Caledonian was destroyed this leads to degradation characteristics if original crude oils are considered. In earlier work, Zhang et al. (2009) also considered different structural zones during a variety of evolutionary phases can influence oil accumulation. These researchers showed that the TZ Number 10 structural zone shared the same accumulation phase as the TZ Number I fault zone, but that the tectonic activity within the structural zone was less than that within the fault zone. This resulted in an intact clastic rock layer which hindered oil migration above the limestone. The advantage of this migration within the TZ Number I fault zone is that oils generated there tend to be more complex in their composition than their counterparts formed within the TZ Number 10 structural zone. These differences also mean that the geochemical characteristics of oils formed within the TZ Number I fault zone tend to vary more widely.

A large number of strike slip faults formed within the TZ area caused marked improvements in the growth of reservoir carbonate voids and stems linking different reservoirs (Wu et al., 2012; Yang et al., 2007; Zhou et al., 2013). At the same time, these strike slip faults controlled the migration and accumulation of oil into reservoirs. Most notably, the end of Silurian-to-early Devonian and late Permian periods were two most active phases of strike slip faults within the Tarim Basin (Jia, 2004). Zhang et al. (2008) reported that middle-to-upper Ordovician gas reservoirs formed by the pyrolysis of paleo-oil accumulations underneath Cambrian salt deposits as the growth of main and strike slip faults provided a number of possibilities for hydrocarbons to migrate upwards. As shown on a geological map of this area (Figure 1), light crude oils within the TZ Number 10 structural zone are mostly located within the boundaries of the main fault while there are more strike slip faults within the TZ Number I fault zone. These smaller faults provided a large number of effective channels connecting different reservoirs and resulted in several phases of oil charging (Li et al., 2006); this range of crude oils with markedly different geochemical characteristics is the cause of the parameter variation seen within this region. Notably, although well ZG46 is located within the TZ Number 10 structural zone, a number of strike slip faults connect it to the TZ Number I fault zone nearby; this might be the cause of several distinct episodes of oil charging. In addition, structures within the Tarim Basin tend to become less active from east-to-west and the ZG46 well is located within the western TZ Number 10 fault, a possible advantage that prevented the degradation of high maturity oils. Indeed, a highly mature oil reservoir in the eastern TZ Number 10 structural zone was destroyed as it lacked good cover even though strike slip faults were present in the vicinity. These structural observations explain why the toluene/MCH ratio of ZG46 oils sample is 3.03, the naphthalene/phenanthrene ratio is 14.71, and the DBT/phenanthrene ratio is 3.91, markedly higher than the values recorded for other oil samples within the TZ Number 10 structural zone.

Geochemical features of toluene and methylcyclohexane in the light crude oils. Regarding the geochemical characterization of toluene and methyl cyclohexane in TZ light crude oils, data demonstrate that saturated ring hydrocarbons can transform into aromatic hydrocarbons by dehydrogenating as maturity gets higher. This is at least one important way in which aromatic hydrocarbons are generated. Several recent studies have shown that alkyl cyclohexane can transform into alkyl benzene series compounds by dehydrogenating (Darwin et al.,

2016a, 2016b). Based on these results, it is supposed that a close evolutionary origin may exist between toluene and methyl cyclohexane in light crude oils, maybe some toluene can be directly derived from methylcyclohexane, and basically in crude oils toluene and methylcyclohexane should have been derived from the same or some likewise structural units of precursor molecules. Thus, during geological evolution process, changes in relative concentration and stable isotope values of toluene and methylcyclohexane can be used to reveal the geochemical characteristics of high mature oils. Therefore, some more discussion has been made to the TZ light crude oils concerning their toluene and methylcyclohexane.

There are more methylcyclohexane than *n*-heptanes in samples from the TZ Number 10 fault zone (Figure 6), which is accordant to the characterization of marine crude oil. But this relationship is different in samples from the TZ Number I fault zone, among which some samples have more methylcyclohexanes while others have more *n*-heptane (Figure 6). These results are accordant to the fact that some light crude oils from the TZ Number I fault zone had contributed to some oil-cracking gas, and then depleted in methylcyclohexane (Hu et al., 2005; Yu et al., 2013), and therefore enriched in toluene showing a higher maturity as shown in Figure 6. Thus, these results reveal that the TZ Number I fault zone had undergone more complicated geological evolution. As discussed above, ZG46 was obviously enriched in toluene because it is at a very special tectonic location, so the ratio between toluene and methylcyclohexane can be used to distinguish depositional environments and differentiate the maturity of light crude oils.

Stable carbon and hydrogen isotope values for toluene and methylcyclohexane in TZ light crude oils are listed in Table 3. Results show that toluene C isotope values in TZ light crude oils range between −32.69‰ and −22.88‰, while H isotope values range between

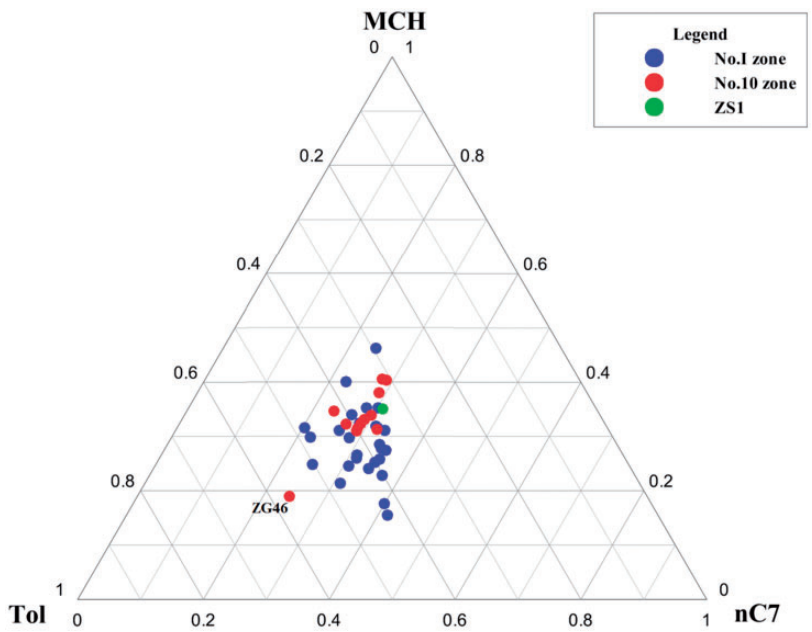

Figure 6. Plot of concentration relationship between *n*-heptane, methylcyclohexane and toluene in Tazhong light crude oil.

Table 3. Stable carbon/hydrogen isotope values of toluene and methylcyclohexane of the light crude oils.

			Toluene		*Methyl cyclohexane*					*Toluene*		*Methyl cyclohexane*	
Well	*Depth (m)*	*Strata*	$\delta^{13}C$	δD	$\delta^{13}C$	δD	*Well*	*Depth (m)*	*Strata*	$\delta^{13}C$	δD	$\delta^{13}C$	δD
ZG10	6198–6309	O	−29.08	−98.72	−29.50	−91.35	ZG432	5131–5520	O	−27.21	−147.10	−26.27	−157.53
ZG101	6998–6309		−29.57	−91.90	−30.12	−84.17	ZG441	5414.38–5522		−29.03	−109.98	−29.94	−124.49
ZG103	6105–6223		−28.33	−96.20	−29.14	−96.29	ZG441-2H	5259.81–5485	O	−28.80	−109.36	−28.98	−108.32
ZG103	6148.44–6233.46	O3	−27.77	−101.54	−29.62	−96.90	ZG44C	5432–5861.50		−29.34	−104.70	−29.00	−109.47
ZG105	5936–6829.28	Oly	−29.87	−94.70	−29.51	−92.92	ZG45	5637.2–5650.17	O3	−29.06	−113.57	−29.96	−120.86
ZG106	6110–6130	O1	−28.86	−101.94	−29.87	−96.75	ZG46	5039.40–5367.34	O3	−32.69	−115.24	−31.31	−125.28
ZG111	6008–6250	O	−28.76	−75.30	−27.50	−74.00	ZG461	5479.64–5745		−28.37	−101.30	−29.05	−114.29
ZG12	6059.58–6279	O	−28.23	−95.95	−28.03	−112.21	ZG461	5475–5745		−28.25	−111.60	−28.06	−119.50
ZG13-1H	5886–7135		−29.44	−70.42	−30.59	−83.49	ZG461	5479.64–5740		−27.39	−110.39	−28.14	−117.46
ZG14-1	6133–6298	O	−29.95	−102.66	−30.12	−111.59	ZG462	5431–5981		−30.04	−114.83	−29.73	−119.57
ZG15	6125–6138	O	−30.22	−78.92	−30.88	−81.36	ZG47	5811–6185		−29.06	−93.69	−29.11	−94.52
ZG151	6083.75–6223.81	O2	−29.68	−110.30	−30.70	−124.80	ZG47CH	6489–6606		−28.91	−102.51	−29.16	−110.56
ZG15-1H	5940–6222.2	Oly	−30.59	−77.50	−29.46	−86.38	ZG48	5498.1–5531.54		−29.33	−104.92	−29.76	−98.80
ZG162	6123–6198	O	−29.90	−114.92	−30.41	−120.19	ZG5	6351.64–6460		−29.38	−98.67	−30.00	−93.28
ZG17	6206–6446	Oly	−29.14	−102.39	−30.00	−88.27	ZG501	6515.5–6790.4		−30.90	−109.41	−30.14	−115.70
ZG17	6438–6448		−27.66	−101.73	−27.28	−96.14	ZG503	5949–6100	Oly	−30.67	−75.08	−31.04	−77.87
ZG17-H1	6088–6887		−29.94	−117.26	−29.66	−120.76	ZG6-2	5937.81–6118	Oly	−28.61	−110.28	−29.13	−127.37
ZG19	6381–6438.5	O	−28.76	−73.08	−30.06	−89.72	ZG6-2	5898.25–6143.17	Oly	−28.52	−116.00	−29.20	−92.18
ZG2	5866–5893	O	−28.44	−72.88	−28.81	−84.77	ZG70	5714–5728		−27.86	−97.48	−29.78	−117.17
ZG22	5605–5736.66	O	−29.87	−111.87	−29.56	−112.68	ZG702	5628–5890	O	−29.52	−101.46	−28.27	−118.80
ZG42	4980.08–5334.09	Oly	−28.72	−106.17	−30.28	−105.20	ZS1	6426–6497	∈	−32.10	−121.49	−32.54	−114.17
ZG43-1	5200–5798	Oly	−29.62	−121.34	−29.84	−124.41							

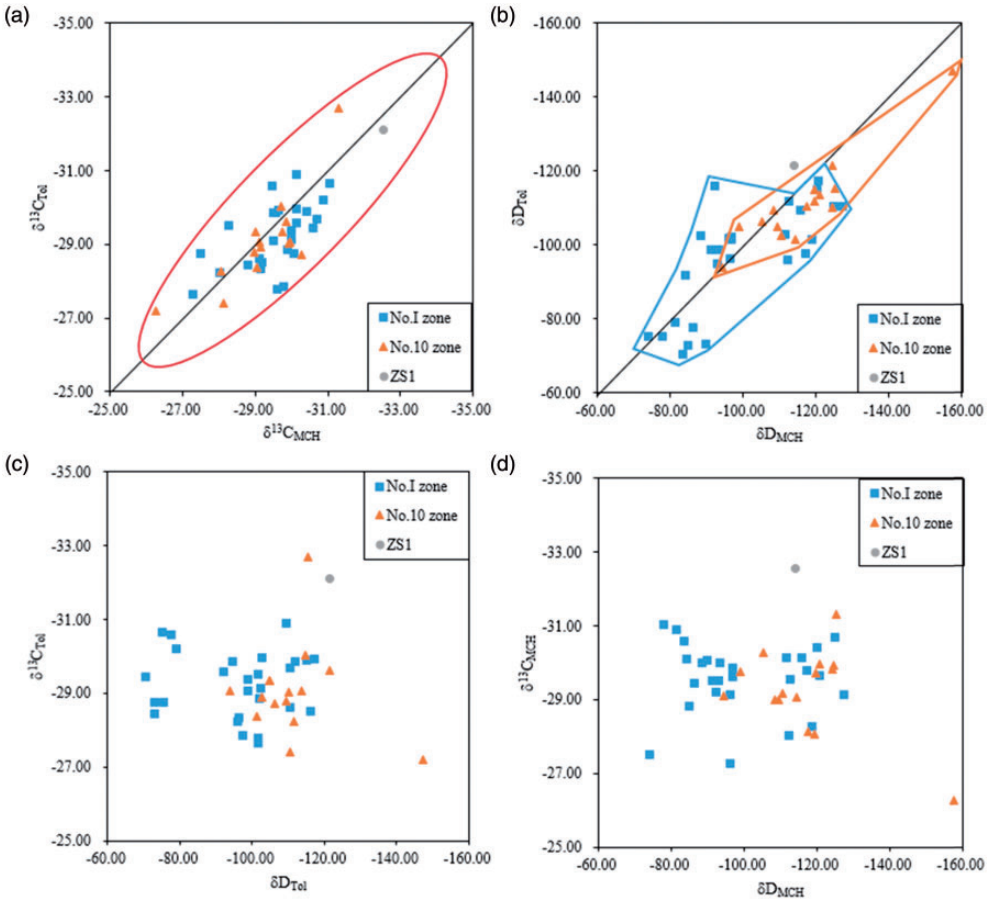

Figure 7. Graphs to show: (A) $\delta^{13}C$ of toluene versus methylcyclohexane; (B) δD of toluene versus methylcyclohexane; (C) $\delta^{13}C$ versus δD of toluene; and (D) $\delta^{13}C$ versus δD of methylcyclohexane in Tazhong light crude oils.

−147.10‰ and −70.42‰. At the same time, methylcyclohexane C isotope values in TZ light crude oils range between −32.54‰ and −26.27‰, while H isotope values range between −157.53‰ and −74.00‰. A positive correlation is also seen between toluene and methyl cyclohexane $\delta^{13}C$ values (Figure 7A). Measured differences in $\delta^{13}C$ between toluene and methyl cyclohexane are mostly within 1‰ of one another, while differences in δD between toluene and methyl cyclohexane are mostly within 10‰. This result, that the isotope values of toluene and methylcyclohexane are close, indicates that these two molecules might share the same precursors or the presence of an inheritance relationship from methylcyclohexane to toluene as discussed above.

The data distribution of $\delta^{13}C$ and δD in toluene and methyl cyclohexane (Figure 7A,B) fall around a line with a slope of 1, while the δD of toluene and methyl cyclohexane in Figure 7(B) fall below this line, especially the samples from TZ Number 10 structural zone. This result suggested that the δD of toluene is generally heavier than those of methyl

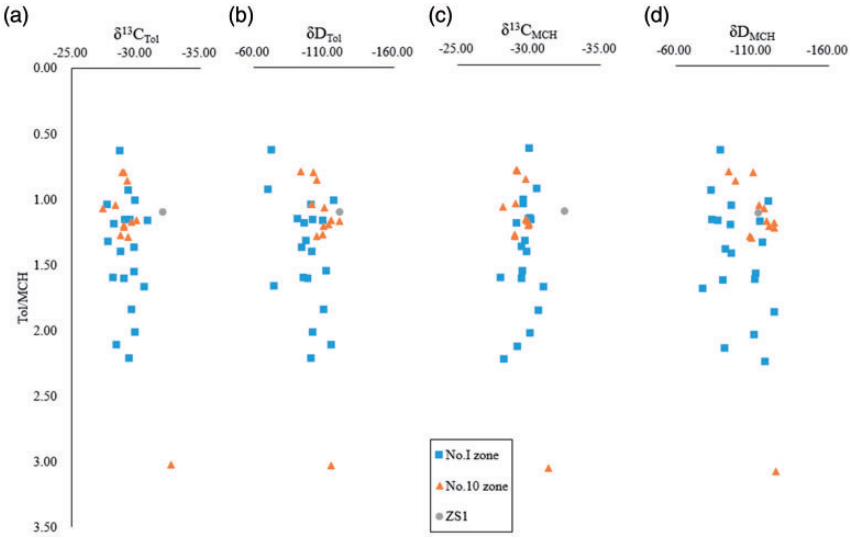

Figure 8. Plots of toluene/methylcyclohexane ratios versus: (A) $\delta^{13}C$ values of toluene; (B) δD values of toluene; (C) $\delta^{13}C$ values of methylcyclohexane; and (D) δD values of methyl cyclohexane in Tazhong light crude oils.

cyclohexane. As discussed above, one important way that aromatic hydrocarbons are generated via the transmutation of saturated ring hydrocarbons in crude oils via dehydrogenation as maturity increases. This will cause the breakage of C–H bonds in the molecule and then enriched in deuterium for toluene.

No distinct correlation between $\delta^{13}C$ and δD in either toluene or methylcyclohexane is evident from the TZ light crude oils, as the former is sensitive to both precursors and depositional environments but less so to thermal evolution, whereas the latter is more sensitive to thermal stress. After oil charging, crude oils containing different kinds of compounds from different charging phases will exhibit different stable isotope features, which will be commingled into the geochemical outcomes of the light crude oils. So in Figure 8 these characteristics are reflected on plots of toluene and methylcyclohexane ratios versus $\delta^{13}C$ and δD in TZ light crude oils. No matter how these ratios vary, no obvious regular pattern is found in our data between toluene and methylcyclohexane and their $\delta^{13}C$ or δD, so long as crude oils contain compounds charged during different geological phases when they were derived from different precursors and depositional environments. However, in the geochemical study on light crude oils, toluene and methylcyclohexane should be investigated in details as they are abundant in the light crude oils and may be with genetic relationships, so further work will be helpful to the study on light crude oils from the composition, stable carbon/hydrogen isotope analyses of toluene and methylcyclohexane.

Conclusions

A total of 89 crude oils were analyzed in this study with emphasis on TZ light crude oil aromatic hydrocarbons from different structural zones. The aim of this study was to evaluate

the geochemical parameters of these crude oils and to investigate their stable carbon/hydrogen isotope ratios.

Results reveal that the crude oils from TZ area are highly mature, especially true for the light crude oils. At high mature stage the normal biomarker parameters are invalid and then the aromatic hydrocarbon compounds are the main study targets in this work. The distribution of aromatic hydrocarbons is different between crude oils from different structural zone. Thus, the MN/DMN, DMN/TMN, MCH/Tol, DBT/phenanthrene, and naphthalene/phenanthrene ratios of crude oils from the TZ Number I fault zone range widely while those from the TZ Number 10 structural zone encompass a relatively narrow range of variation. This difference highlights the fact that the TZ Number I fault zone experienced more intense structural movements than the TZ Number 10 structural zone. The former also formed a more effective migration pathway as a result; thus, the crude oils that formed within the TZ Number I fault zone have undergone several charging phases and are more complicated in composition.

The distribution of stable carbon/hydrogen isotope values revealed by this study indicates a relationship between the origin of toluene and methylcyclohexane. Toluene can be derived from the dehydrogenation of methylcyclohexane in crude oils. Nevertheless, the ratios of toluene and methylcyclohexane are complicated within the TZ area and no regular pattern is evident due to multiple charging events and the complex geological evolution of the TZ area. The results of this study nevertheless reveal that the geochemical characteristics and significance of toluene and methylcyclohexane in light crude oils are worthy of further study.

Declaration of conflicting interests

The author(s) declared no potential conflicts of interest with respect to the research, authorship, and/or publication of this article.

Funding

The author(s) disclosed receipt of the following financial support for the research, authorship and/or publication of this article: This work was financially supported by the National Natural Science Foundation of China (Grant No. 41472109), the Strategic Priority Research Program of the Chinese Academy of Sciences (XDA14010103) and the National Oil and Gas Project of China (2017ZX05008002).

References

Chakhmakhchev A, Suzuki M and Takayama K (1997) Distribution of alkylated dibenzothiophenes in petroleum as a tool for maturity assessments. *Organic Geochemistry* 26(7): 483–490.

Chang XC, Wang TG, Li QM, et al. (2013) Charging of Ordovician reservoirs in the Halahatang depression (Tarim Basin, NW China) determined by oil geochemistry. *Journal of Petroleum Geology* 36(4): 383–398.

Darwin AR, Françoise B, Roda B, et al. (2016a) Thermal cracking of n-butylcyclohexane at high pressure (100 bar) – Part 1: Experimental study. *Journal of Analytical and Applied Pyrolysis* 117: 1–16.

Darwin AR, Françoise B, Roda B, et al. (2016b) Thermal cracking of n-butylcyclohexane at high pressure (100 bar) – Part 2: Mechanistic modeling. *Journal of Analytical and Applied Pyrolysis* 120: 174–185.

Dzou LIP, Noble RA and Senftle JT (1995) Maturation effects on absolute biomarker concentration in a suite of coals and associated vitrinite concentrates. *Organic Geochemistry* 23: 681–697.

Han WX, Tao SZ, Hu GY, et al. (2017) Light hydrocarbon geochemical characteristics and their application in Upper Paleozoic, Shenmu gas field, Ordos Basin. *Energy Exploration & Exploitation* 35(1): 103–121.

Hanson AD, Zhang SC, Moldowan JM, et al. (2000) Molecular organic geochemistry of the Tarim Basin, Northwest China. *AAPG Bulletin* 84(8): 1109–1128.

He ZL, Jin XH, Wo YJ, et al. (2016) Hydrocarbon accumulation characteristics and exploration domains of ultra-deep marine carbonates in China. *China Petroleum Exploration* 21(2): 3–14.

Hu GY, Xiao ZR, Luo X, et al. (2005) Light hydrocarbon composition difference between two kinds of cracked gases and its application. *Natural Gas Industry* 25(9): 23–25.

Hu SZ, Wilkes H, Horsfield B, et al. (2016) On the origin, mixing and alteration of crude oils in the Tarim Basin. *Organic Geochemistry* 97: 17–34.

Huang HP, Zhang SC, Su J (2016) Palaeozoic oilsource correlation in the Tarim Basin, NW China: A review. *Organic Geochemistry* 94: 32–46.

Huang HP, Zhang SC, Gu Y, et al. (2017) Impacts of source input and secondary alteration on the extended tricyclic terpane ratio: A case study from Palaeozoic sourced oils and condensates in the Tarim Basin, NW China. *Organic Geochemistry* 112: 158–169.

Jia CZ (2004) *Plate Tectonics and Continental Dynamics in the Tarim Basin*. Beijing: Petroleum Industry Press.

Jin ZJ (2005) Particularity of petroleum exploration on marine carbonate strata in China sedimentary basins. *Earth Science Frontiers* 12(3): 15–22.

Li MJ, Hu SH, Wang QG, et al. (2006) Discovery of strike-slip fault system in Tazhong area and geologic meaning. *OGP* 41(1): 116–121.

Li MJ and Wang TG (2005) The generating mechanism of methylated naphthalene series in crude oils and the application of their maturity parameters. *Petroleum Geology and Experiment* 27(6): 606–611.

Liang DG and Chen JP (2005) Oil-source correlations for high and over matured marine source rocks in south China. *Petroleum Exploration and Development* 32(2): 8–14.

Liang DG, Zhang SC, Zhang BM, et al. (2000) Understanding on marine oil generation in China based on Tarim Basin. *Earth Science Frontiers* 7: 533–547.

Liu N, Qiu NS, Chang J, et al. (2017) Quantitative fluorescence techniques for investigating hydrocarbon charge history in carbonate reservoir. *Energy Exploration & Exploitation* 35(3): 356–375.

Liu D, Yu C, Huang SP, et al. (2015) Using light hydrocarbons to identify the depositional environment of source rocks in the Ordos Basin, central China. *Energy Exploration & Exploitation* 33(6): 869–890.

Luo J, Cheng KP, Fu LX, et al. (2001) Alkylated dibenzothiophene index – A new method to assess thermal maturity of source rocks. *Acta Petrolei Sinica* 22(3): 27–31.

Price LC (1993) Thermal stability of hydrocarbons in nature: Limits, evidence, characteristics, and possible control. *Geochimica et Cosmochimica Acta* 57: 3261–3280.

Qiu NS, Chang J, Zuo YH, et al. (2012) Thermal evolution and maturation of Lower Paleozoic source rocks in the Tarim Basin, northwest China. *AAPG Bulletin* 96(5): 789–821.

Qiu NS, Jin ZJ and Wang FY (1997) The effect of the complex geothermal field based on the multi-structure evolution to hydrocarbon generation – A case of Tazhong area in Tarim Basin. *Acta Sedimentologica Sinica* 15(2): 142–144.

Qiu NS, Wang JY, Mei QH, et al. (2010) Constraints of (U–Th)/He ages on Early Paleozoic tectonothermal evolution of the Tarim Basin, China. *Science in China* 53: 964–976.

Radke M, Welte DH and Willsch H (1982) Geochemical study on a well in the western Canada Basin: Relation of the aromatic distribution pattern to maturity of organic matter. *Geochimica et Cosmochimica Acta* 46: 1–10.

Santamaría-Orozco D, Horsfield B, Di Primio R, et al. (1998) Influence of maturity on distributions of benzo and dibenzothiophenes in Tithonian source rocks and crude oils, Sonda de Campeche, Mexico. *Organic Geochemistry* 28(7–8): 423–439.

Sun YG, Xu SP, Lu H, et al. (2003) Source facies of the Paleozoic petroleum systems in the Tabei uplift, Tarim Basin, NW China: Implications from aryl isoprenoids in crude oils. *Organic Geochemistry* 34(4): 629–634.

Wang ZM, Xie HW, Chen YQ, et al. (2014) Discovery and exploration of Cambrian subsalt dolomite original hydrocarbon reservoir at Zhongshen-1 well in Tarim Basin. *China Petroleum Exploration* 19(2): 1–13.

Wang M, Zhu GY, Ren LM, et al. (2015) Separation and characterization of sulfur compounds in ultra-deep formation crude oils from Tarim Basin. *Energy & Fuels* 29: 4842–4849.

Wu GH, Yang HJ, Qu TL, et al. (2012) The fault system characteristics and its controlling roles on marine carbonate hydrocarbon in the Central Uplift, Tarim Basin. *Acta Petrologica Sinica* 28(3): 793–805.

Xing QY, Pei WW, Xu RQ, et al. (2005) *Basic Organic Chemistry*. Beijing: Higher Education Press, pp. 444–448.

Yang HJ, Hao F, Han JF, et al. (2007) Fault systems and multiple oil-gas accumulation play of the Lunnan Lower Uplift, Tarim Basin. *Chinese Journal of Geology* 42(4): 795–811.

Yang HJ, Zhu GY, Han JF, et al. (2011) Conditions and mechanism of hydrocarbon accumulation in large reef-bank karst oil/gas fields of Tazhong area, Tarim Basin. *Acta Petrologica Sinica* 27(6): 1865–1885.

Yu C, Tian XW and Li J (2013) The characteristics of light hydrocarbon in oil-associated gas and its application in platform area of Tarim Basin. *Natural Gas Geoscience* 24(4): 774–783.

Yun JB, Jin ZJ and Xie GJ (2014) Distribution of major hydrocarbon source rocks in the Lower Paleozoic, Tarim Basin. *Oil and Gas Geology* 35(6): 827–838.

Zhang SC, Hanson AD, Moldowan JM, et al. (2000) Paleozoic oil-source rock correlations in the Tarim Basin, NW China. *Organic Geochemistry* 31: 273–286.

Zhang SC and Huang HP (2005) Geochemistry of Palaeozoic marine petroleum from the Tarim Basin, NW China: Part 1. Oil family classification. *Organic Geochemistry* 36(8): 1204–1214.

Zhang SC, Huang HP, Su J, et al. (2015a) Ultra-deep liquid hydrocarbon exploration potential in cratonic region of the Tarim Basin inferred from gas condensate genesis. *Fuel* 160: 583–595.

Zhang SC, Huang HP, Su J, et al. (2015b) Geochemistry of Paleozoic marine petroleum from the Tarim Basin, NW China: Part 5. Effect of maturation, TSR and mixing on the occurrence and distribution of alkyldibenzothiophenes. *Organic Geochemistry* 86: 5–18.

Zhang SC, Liang DG, Zhang BM, et al. (2004) *Marine Hydrocarbon Generation in Tarim Basin*. Beijing: Petroleum Industry Press, p. 178.

Zhang ZP, Wang Y, Yun JB, et al. (2009) Control of fault at different evolution stages on hydrocarbon accumulation in Tazhong area, the Tarim Basin. *Oil and Gas Geology* 30(3): 316–323.

Zhang CZ, Yu HF, Zhang HZ, et al. (2008) Characteristic, genesis geologic meaning of strike-slipfault system in Tazhong area. *Journal of South-West Petroleum University (Science and Technology Edition)* 34(5): 22–26.

Zhang SC, Zhang BM, Li BL, et al. (2011) History of hydrocarbon accumulations spanning important tectonic phases in marine sedimentary basins of China: Taking the Tarim Basin as an example. *Petroleum Exploration and Development* 38(2): 8–14.

Zhang SC, Zhang B, Yang HJ, et al. (2012) Adjustment and alteration of hydrocarbon reservoirs during the Late Himalayan period, Tarim Basin, NW China. *Petroleum Exploration and Development* 39(6): 668–680.

Zhao ZJ, Zhou XY, Zheng XP, et al. (2005) Evidence of chief source rock in Tarim Basin. *Acta Petrolei Sinica* 26(3): 10–15.

Zhao WZ, Zhu GY, Su J, et al. (2012) Study on the multi-stage charging and accumulation model of Chinese marine petroleum: Example from eastern Lungu area in the Tarim Basin. *Acta Petrologica Sinica* 28(3): 709–721.

Zhou SX, Jia XL, Song ZX, et al. (2008) Aromatic compositions of different occurrence states in deep carbonate rocks from Tarim Basin. *Acta Sedimentologica Sinica* 26(2): 330–339.

Zhou XY, Lü XX, Yang HJ, et al. (2013) Effect of strike-slip faults on the differential enrichment of hydrocarbons in the northern slope of Tazhong area. *Acta Petrolei Sinica* 34(4): 628–637.

Zhu GY, Liu XW, Zheng DM, et al. (2015) Geology and hydrocarbon accumulation of the large ultra-deep Rewapu oilfield in Tarim basin, China. *Energy Exploration & Exploitation* 33(2): 123–144.

Zhuo GM and Wang JJ (1999) Analysis of petroleum geology in Tazhong region. *Acta Petrolei Sinica* 20(4): 1–6.